Semi-Empirical Prediction of Noise from Non-Zero Pressure Gradient Turbulent Boundary Layers

S. A. E. Miller

University of Florida
Department of Mechanical and Aerospace Engineering
Theoretical Fluid Dynamics and Turbulence Group

saem@ufl.edu
https://faculty.eng.ufl.edu/fluids

Outline

- Introduction and Background
- Mathematical Theory
- Results
  - Flow
  - Aeroacoustics
- Summary and Conclusion

Introduction and Background

Turbulent Boundary Layers

Present within almost all flow-fields of aerospace flight vehicles

This paper based on recent publication - Miller, S. A. E., "Prediction of Turbulent Boundary-Layer Noise," AIAA Journal, 2017. doi:10.2514/1.J055087.

Objective: Develop acoustic analogy for prediction of TBL noise with NZPG

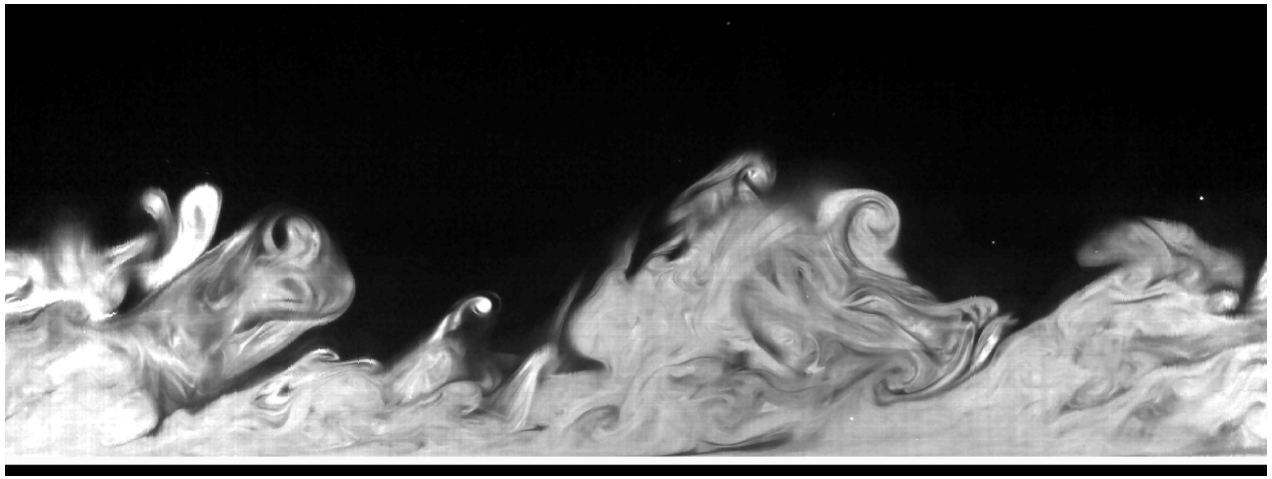

Lee, J. H., Kwon, Y. S., Monty, J. P., and Hutchins, N., "Tow-Tank Investigation of the Developing Zero-Pressure-Gradient Turbulent Boundary Layer," 18th Australasian Fluid Mechanics Conference, 2012.

Previous Investigations (Select)
Boundary Layers with Pressure Gradients

- Investigations focusing on turbulence with NZPG are rare
- Scaling statistics of turbulence in NZPG TBL is an open problem
- Kovasznay (1970) characterizes pressure gradient using a non-dimensional approach

$$K = \nu(\rho u_\infty^3)^{-1}\partial p/\partial x$$

- Kline (1967) examined mean velocity profiles of various boundary layers characterized by K
- Castillo (1997), collapsed the meanflow for pipes and channel flows using power laws and showed collapse possible
  - Opens possibility of correctly predicting boundary layer meanflow with a pressure gradient
  - No insight on effect of pressure gradient on turbulent statistics

Previous Investigations (Select) Boundary Layers with Pressure Gradients - Aeroacoustics

- Powell (1960) used Lighthill's acoustic analogy in conjunction with mirror source and showed that acoustic power is proportional to volumetric integral of second time derivative of Lighthill stress tensor multiplied by $\rho_\infty^{-1} c_\infty^{-5}$
- Powell showed that pressure on wall is an aerodynamic imprint of turbulence and Naka et al. (2015) supported this viewpoint
- Howe (1991) related the wall wavenumber pressure spectrum to the acoustic spectrum
- Glegg et al. (2007) created a model that depends on the wavenumber spectrum of the surface pressure fluctuations
- Hu et al. (2003, 2006), performed DNS combined with an acoustic analogy and a half-space Green's function
- Gloerfelt and Berland (2013) and Gloerfelt and Margnat (2014) performed LES of compressible turbulent boundary layer at three high speed Mach numbers. Predictions showed excellent agreement but had considerable computational cost
- Miller (2017) used an acoustic analogy with mathematical models of the source terms to predict noise from turbulent boundary layers using an acoustic analogy and the results agreed excellently with Gloerfelt and Berland (2013) and Gloerfelt and Margnat (Gloerfelt2014)

Previous Scaling Analysis

Previous paper of Miller (AIAAJ 2017) we have showed scaling of TBL noise goes as

$$S \propto c_f^2 \overline{\rho}^2 \left(\frac{\rho_\infty}{\rho_w} \right)^2 l_{sx} l_{sy} l_{sz} \tau_s \left\{ \frac{\overline{u}^4 u_\infty^4}{c_\infty^4 r^2 l_{sx}^4} + \frac{\overline{u}^2 u_\infty^4}{c_\infty^2 r^4 l_{sx}^2} + \frac{u_\infty^4}{r^6} \right\} V$$

and within the far-field as

$$S_{\text{far-field}} \propto \frac{1}{r^2} \frac{c_f^2}{c_\infty^4} \frac{\tau_s}{\delta} \left(\frac{\overline{\rho} \rho_\infty}{\rho_w} \right)^2 u_\infty^8 V$$

Mathematical Theory

Theoretical Approach

Lighthill's acoustic analogy,

$$\frac{\partial^2 \rho}{\partial t^2} - c_\infty^2 \frac{\partial^2 \rho}{\partial x_i \partial x_i} = \frac{\partial^2 T_{ij}}{\partial x_i \partial x_j}$$

We solve, expand, convert to pressure, simplify, and obtain,

$$p\left(\boldsymbol{x}, t\right) = \frac{1}{4\pi} \int_{-\infty}^{\infty} \int_{-\infty}^{\infty} \int_{-\infty}^{\infty} \frac{r_i r_j}{r^2} \left[\frac{\ddot{T}_{ij}}{c_\infty^2 r} + \frac{3(1-M_\infty^2)\dot{T}_{ij}}{c_\infty r^2} + \frac{3(1-M_\infty^2)^2 T_{ij}}{r^3} \right]$$
$$- \frac{2 r_i M_{\infty,j}}{r} \left[\frac{2\dot{T}_{ij}}{c_\infty r^2} + \frac{3(1-M_\infty)^2 T_{ij}}{r^3} \right]$$
$$- \delta_{ij} \left[\frac{\dot{T}_{ij}}{c_\infty r^2} + \frac{(1-M_\infty^2) T_{ij}}{r^3} \right]$$
$$+ 2 M_{\infty,i} M_{\infty,j} \frac{T_{ij}}{r^3} d\boldsymbol{\eta}$$

where,

$$r = |\boldsymbol{x} - \boldsymbol{y}| + \boldsymbol{M}_\infty \cdot (\boldsymbol{x} - \boldsymbol{y}) \qquad \text{and,} \qquad \boldsymbol{y} = \boldsymbol{\eta} - c_\infty \boldsymbol{M}_\infty t + \boldsymbol{M}_\infty |\boldsymbol{x} - \boldsymbol{y}|$$

Theoretical Approach

Forced to take a statistical approach…
We perform the two-point cross-correlation of p at x and x' and t and t'

$$\overline{p\left(\boldsymbol{x},t\right)p\left(\boldsymbol{x}',t'\right)}=\frac{1}{16\pi^2}\int_{-\infty}^{\infty}\ldots\int_{-\infty}^{\infty}\left(A_1+A_2+A_3+A_4\right)d\boldsymbol{\eta}'d\boldsymbol{\eta},$$

where for example,

$$\begin{aligned}A_1=&\\ &\frac{r_ir_jr'_lr'_m}{r^2r'^2}\overline{\left[\frac{\ddot{T}_{ij}}{c_\infty^2r}+\frac{3(1-M_\infty^2)\dot{T}_{ij}}{c_\infty r^2}+\frac{3(1-M_\infty^2)^2T_{ij}}{r^3}\right]\left[\frac{\ddot{T}'_{lm}}{c_\infty^2r'}+\frac{3(1-M_\infty^2)\dot{T}'_{lm}}{c_\infty r'^2}+\frac{3(1-M_\infty^2)^2T'_{lm}}{r'^3}\right]}\\ &-\frac{2r_ir_j}{rr}\frac{r'_lM_{\infty,m}}{r'}\overline{\left[\frac{\ddot{T}_{ij}}{c_\infty^2r}+\frac{3(1-M_\infty^2)\dot{T}_{ij}}{c_\infty r^2}+\frac{3(1-M_\infty^2)^2T_{ij}}{r^3}\right]\left[\frac{2\dot{T}'_{lm}}{c_\infty r'^2}+\frac{3(1-M_\infty)^2T'_{lm}}{r'^3}\right]}\\ &-\frac{r_ir_j}{r^2}\delta_{lm}\overline{\left[\frac{\ddot{T}_{ij}}{c_\infty^2r}+\frac{3(1-M_\infty^2)\dot{T}_{ij}}{c_\infty r^2}+\frac{3(1-M_\infty^2)^2T_{ij}}{r^3}\right]\left[\frac{\dot{T}'_{lm}}{c_\infty r'^2}+\frac{(1-M_\infty^2)T'_{lm}}{r'^3}\right]}\\ &+\frac{2r_ir_j}{r^2}\frac{M_{\infty,l}M_{\infty,m}}{r'^3}\overline{\left[\frac{\ddot{T}_{ij}}{c_\infty^2r}+\frac{3(1-M_\infty^2)\dot{T}_{ij}}{c_\infty r^2}+\frac{3(1-M_\infty^2)^2T_{ij}}{r^3}\right]T'_{lm}}\end{aligned}$$

and unfortunately A_2, A_3, and A_4 are just as complicated!

Theoretical Approach

We now group terms according to their contribution to the far-field, mid-field, and near-field,

$$\overline{p\left(\boldsymbol{x},t\right)p\left(\boldsymbol{x}',t'\right)}=\frac{1}{16\pi^2}\int_{-\infty}^{\infty}...\int_{-\infty}^{\infty}F_t\overline{\ddot{T}_{ij}\ddot{T}'_{lm}}+M_t\overline{\dot{T}_{ij}\dot{T}'_{lm}}+N_t\overline{T_{ij}T'_{lm}}d\boldsymbol{\eta}'d\boldsymbol{\eta},$$

where the far-field term is,

$$F_t=\frac{r_ir_jr'_lr'_m}{r^2r'^2}\left[\frac{1}{c_\infty^4rr'}\right]$$

and the mid-field term is,

$$\begin{aligned}M_t=&\frac{r_ir_jr'_lr'_m}{r^2r'^2}\left[\frac{9(1-M_\infty^2)^2}{c_\infty^2r^2r'^2}-\frac{3(1-M_\infty^2)^2}{c_\infty^2rr'^3}-\frac{3(1-M_\infty^2)^2}{c_\infty^2r^3r'}\right]\\&-\frac{r_ir_jr'_l}{r^2r'}\left[\frac{6(1-M_\infty^2)}{c_\infty^2}\left(\frac{2M_{\infty,m}}{r^2r'^2}-\frac{M_{\infty,m}}{rr'^3}\right)\right]-\frac{r_ir'_lr'_m}{rr'^2}\left[\frac{6(1-M_\infty^2)}{c_\infty^2}\left(\frac{2M_{\infty,j}}{r^2r'^2}-\frac{M_{\infty,j}}{r^3r'}\right)\right]\\&-\frac{r_ir_j}{r^2}\left[\frac{3(1-M_\infty^2)\delta_{lm}}{c_\infty^2r^2r'^2}+\frac{(1-M_\infty^2)\delta_{lm}}{c_\infty^2rr'^3}+\frac{2M_{\infty,l}M_{\infty,m}}{c_\infty^2rr'^3}\right]\\&-\frac{r'_lr'_m}{r'^2}\left[\frac{3(1-M_\infty^2)\delta_{ij}}{c_\infty^2r^2r'^2}+\frac{(1-M_\infty^2)\delta_{ij}}{c_\infty^2r^3r'}+\frac{2M_{\infty,i}M_{\infty,j}}{c_\infty^2r^3r'}\right]\\&+\frac{r_ir'_l}{rr'}\left[\frac{16M_{\infty,j}M_{\infty,m}}{c_\infty^2r^2r'^2}\right]+\frac{r_i}{r}\left[\frac{4M_{\infty,j}\delta_{lm}}{c_\infty^2r^2r'^2}\right]+\frac{r'_l}{r'}\left[\frac{4M_{\infty,m}\delta_{ij}}{c_\infty^2r^2r'^2}\right]+\frac{\delta_{ij}\delta_{lm}}{c_\infty^2r^2r'^2}\end{aligned}$$

The near-field term is even larger.

Two-Point Cross-Correlation

The model integrations are based upon the mixed Gaussian-exponentially decaying model of the two-point cross-correlation of the equivalent source

$$R = \exp\left[-\frac{(\xi - \overline{u}\tau)^2}{l_{sx}^2}\right] \exp\left[-\frac{(1 - \tanh[\alpha|\xi|])|\xi - \overline{u}\tau|}{l_{sx}}\right] \exp\left[-\frac{|\xi|}{l_{sx}}\right] \exp\left[-\frac{|\eta|}{l_{sy}}\right] \exp\left[-\frac{|\zeta|}{l_{sz}}\right]$$

We estimate the length scale within *R* by adopting the model of Efimtsov (1982)

$$l_s = a_4 \delta \left[\left(\frac{2\pi a_1 f}{u_c} \right)^2 + \frac{a_2^2}{\left(\frac{2\pi f \delta}{u_\tau} \right)^2 + \left(\frac{a_2}{a_3} \right)^2} \right]^{-\frac{1}{2}}$$

where $a_1 = 0.1$, $a_2 = 72.8$, $a_3 = 1.54$, and $a_4 = 6$. The spanwise length scale uses an alternative set of coefficients, where $a_1 = 0.1$, $a_2 = 548$, $a_3 = 13.5$, and other values of a_i remain the same

Final Model Equation

The spectral density of acoustic pressure is

$$S\left(\boldsymbol{x},\omega\right)=4\pi^{-2}\int_{-\infty}^{\infty}\ldots\int_{-\infty}^{\infty}\left\{A_{ijlm}l_{sy}l_{sz}F_{t}\mathcal{I}\right\}d\xi d\boldsymbol{\eta}$$

The coefficient matrix A_{ijlm} is

$$A_{ijlm}\approx\mathcal{P}_{f}\overline{\rho}\;\overline{\rho}'\overline{u_{i}u_{j}}\;\overline{u_{l}'u_{m}'},$$

and

$$\mathcal{I}=\begin{cases}\frac{12\overline{u}^{4}}{l_{sx}^{4}}\frac{\pi^{1/2}l_{sx}}{2\overline{u}}\exp\left[\frac{\overline{u}^{2}-2i\overline{u}(l_{sx}+2\pi)\omega-l_{sx}^{2}\omega^{2}+\overline{u}\tanh[\alpha\xi](-2(\overline{u}+il_{sx}\omega)+\overline{u}\tanh[\alpha\xi])}{4\overline{u}^{2}}\right]\\ \times\left(\exp\left[\frac{il_{sx}\omega\tanh[\alpha\xi]}{\overline{u}}\right]\operatorname{erfc}\left[\frac{\overline{u}-il_{sx}\omega-\overline{u}\tanh[\alpha\xi]}{2\overline{u}}\right]+\exp\left[\frac{il_{sx}\omega}{\overline{u}}\right]\operatorname{erfc}\left[\frac{\overline{u}+il_{sx}\omega-\overline{u}\tanh[\alpha\xi]}{2\overline{u}}\right]\right) & \text{for } \xi\geq 0\\ \text{and}\\ \frac{12\overline{u}^{4}}{l_{sx}^{4}}\frac{\pi^{1/2}l_{sx}}{2\overline{u}}\exp\left[\frac{\overline{u}^{2}-2i\overline{u}(l_{sx}+2\pi)\omega-l_{sx}^{2}\omega^{2}+\overline{u}\tanh[\alpha\xi](2(\overline{u}-il_{sx}\omega)+\overline{u}\tanh[\alpha\xi])}{4\overline{u}^{2}}\right]\\ \times\left(\operatorname{erfc}\left[\frac{\overline{u}-il_{sx}\omega+\overline{u}\tanh[\alpha\xi]}{2\overline{u}}\right]+\exp\left[\frac{il_{sx}\omega(1+\tanh[\alpha\xi])}{\overline{u}}\right]\operatorname{erfc}\left[\frac{\overline{u}+il_{sx}\omega+\overline{u}\tanh[\alpha\xi]}{2\overline{u}}\right]\right) & \text{for } \xi<0.\end{cases}$$

FUN3D Steady RANS Simulations

- NASA Langley FUN3D Solver
- 40k iterations per flow-field
- Closed by Wilcox Reynolds stress model
- Mach number 0.3, 0.5, 0.7, and 0.9
- Pressure gradient imposed within the flow through

$$\partial \tilde{p}/\partial x = \nu(\rho u_\infty^3)^{-1}\partial p/\partial x$$

- Imposed via term placement on RHS of momentum equation
- Resultant pressure gradient found numerically from solution

Evaluation of Spectral Density

- The final equation does not directly account for the wall
- We adopt the approach used by Powell (1960), who used the concept of the `mirror' source
- Sources reside within the turbulent flow-field
- There is an acoustic propagation delay from the mirror source
- Numerical integration is performed using the CFD solution

Results

Flow-Conditions

Theory based flow conditions

$\mathcal{M}_\infty$	$\mathcal{R}e_x$	x_l [m]	τ_w [Pa]	δ [m]	u_τ [ms^{-1}]	y^+ Distance [m]
0.30	6.818×10^{6}	1	20.43	3.073×10^{-2}	4.117	3.667×10^{-6}
0.50	1.136×10^{7}	1	53.24	2.976×10^{-2}	6.646	2.271×10^{-6}
0.70	1.591×10^{7}	1	100.2	2.916×10^{-2}	9.116	1.656×10^{-6}
0.90	2.045×10^{7}	1	160.7	2.872×10^{-2}	11.55	1.307×10^{-6}

Steady RANS inlet boundary conditions

$\mathcal{M}_\infty$	$p_t p_\infty^{-1}$	$T_t T_\infty^{-1}$
0.30	1.06443	1.01800
0.50	1.18621	1.05000
0.70	1.38710	1.09800
0.90	1.69130	1.16200

Numerically Derived Flow Properties

$\mathcal{M}_\infty$	$\mathcal{R}e_x$	x_l [m]	τ_w [Pa]	δ [m]	u_τ [ms^{-1}]	y^+ Distance [m]	$\partial\tilde{p}/\partial x$	$\partial p/\partial x$ [Pa m$^-$
0.30	6.818×10^6	1	12.512	7.792×10^{-3}	3.223	4.683×10^{-6}	0	-12
0.30	6.818×10^6	1	21.812	2.709×10^{-3}	4.282	3.525×10^{-6}	0.01	336
0.30	6.818×10^6	1	30.531	5.957×10^{-3}	5.089	2.966×10^{-6}	0.02	346
0.30	6.818×10^6	1	2.7360	1.170×10^{-2}	1.493	1.010×10^{-5}	-0.01	-770
0.30	6.818×10^6	1	2.4245	9.896×10^{-5}	1.401	1.077×10^{-5}	-0.02	-2855
0.50	1.136×10^7	1	36.468	4.388×10^{-3}	5.528	2.730×10^{-6}	0	-21
0.50	1.136×10^7	1	45.299	4.314×10^{-3}	6.204	2.433×10^{-6}	0.01	272
0.50	1.136×10^7	1	53.394	4.250×10^{-3}	6.771	2.229×10^{-6}	0.02	450
0.50	1.136×10^7	1	30.283	4.499×10^{-3}	5.039	2.995×10^{-6}	-0.01	-483
0.50	1.136×10^7	1	22.445	4.762×10^{-3}	4.322	3.492×10^{-6}	-0.02	-828
0.70	1.591×10^7	1	71.474	2.624×10^{-3}	7.853	1.923×10^{-6}	0	-29
0.70	1.591×10^7	1	79.688	2.677×10^{-3}	8.357	1.807×10^{-6}	0.01	149
0.70	1.591×10^7	1	87.488	2.721×10^{-3}	8.816	1.713×10^{-6}	0.02	251
0.70	1.591×10^7	1	66.807	2.583×10^{-3}	7.622	1.981×10^{-6}	-0.01	-756
0.70	1.591×10^7	1	61.686	2.558×10^{-3}	7.341	2.057×10^{-6}	-0.02	-1250
0.90	2.045×10^7	1	117.434	1.976×10^{-3}	10.398	1.452×10^{-6}	0	-26
0.90	2.045×10^7	1	124.998	1.990×10^{-3}	10.823	1.395×10^{-6}	0.01	13
0.90	2.045×10^7	1	133.133	7.066×10^{-4}	11.394	1.326×10^{-6}	0.02	939
0.90	2.045×10^7	1	112.932	1.968×10^{-3}	10.247	1.473×10^{-6}	-0.01	-1288
0.90	2.045×10^7	1	108.354	1.963×10^{-3}	10.084	1.497×10^{-6}	-0.02	-2352

Computational Domain

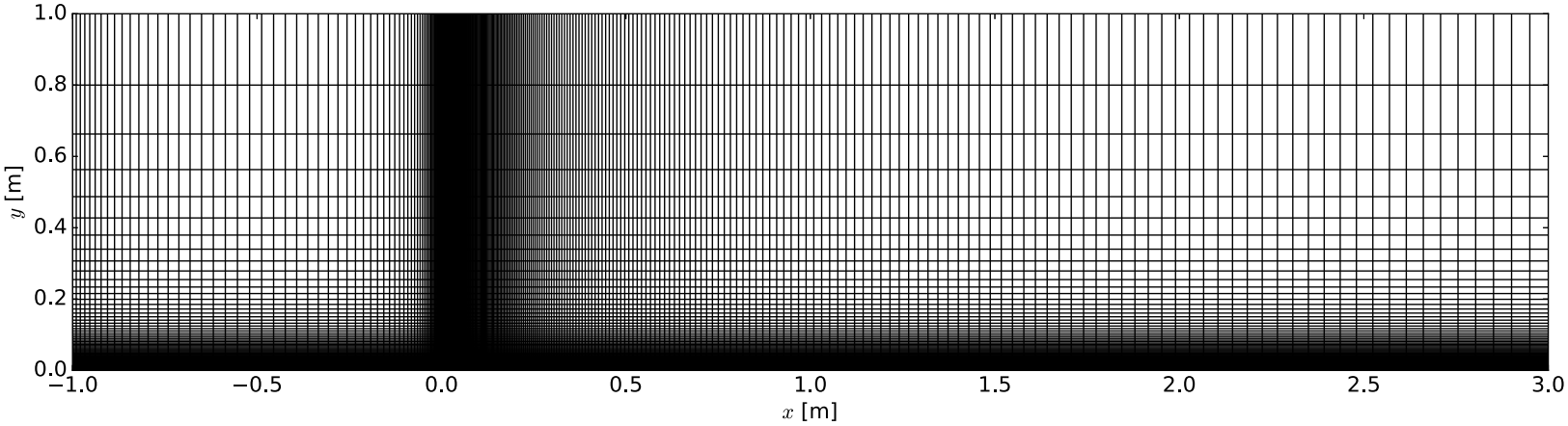

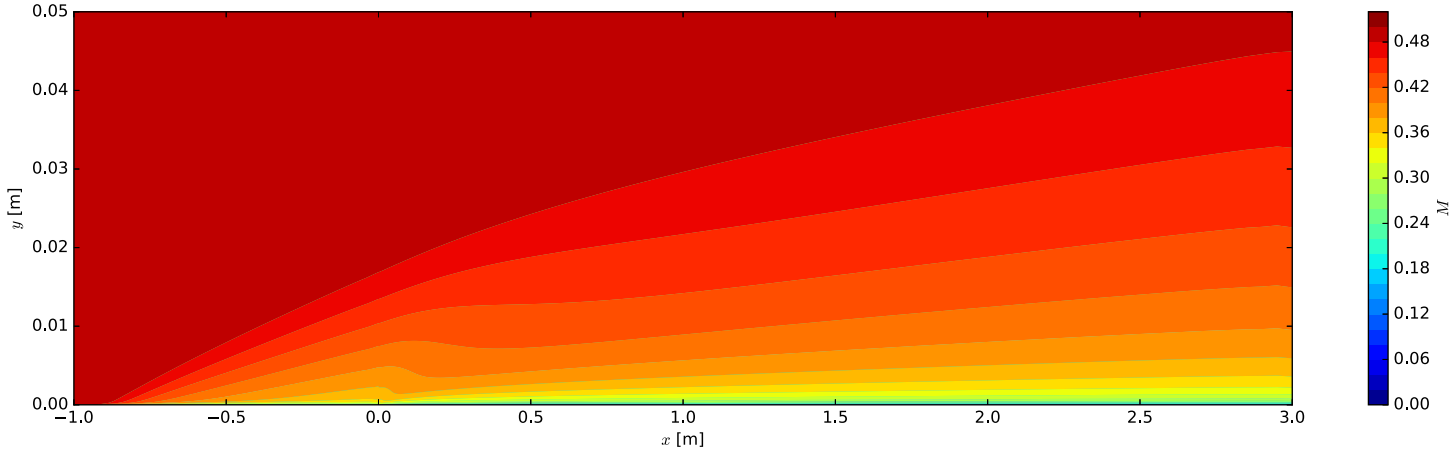

Contours of M for $M_\infty = 0.50$ and $\partial \tilde{p}/\partial x = 0$

Example Residual History

Variation of residual of field-variables for $M_\infty = 0.90$ and $\partial p'/\partial x = 0$.

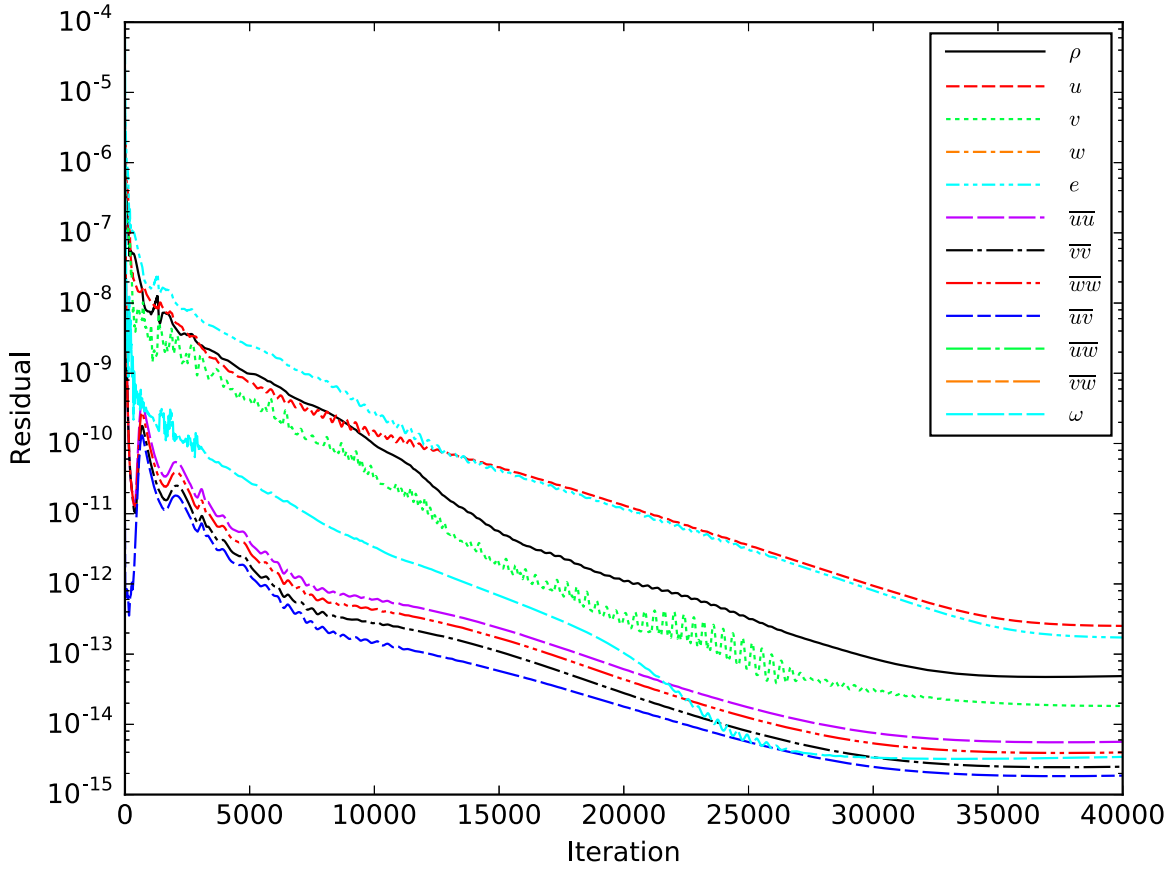

Variation of u^+ in Inner Coordinates as Function of M_∞ and $\partial\tilde{p}/\partial x$

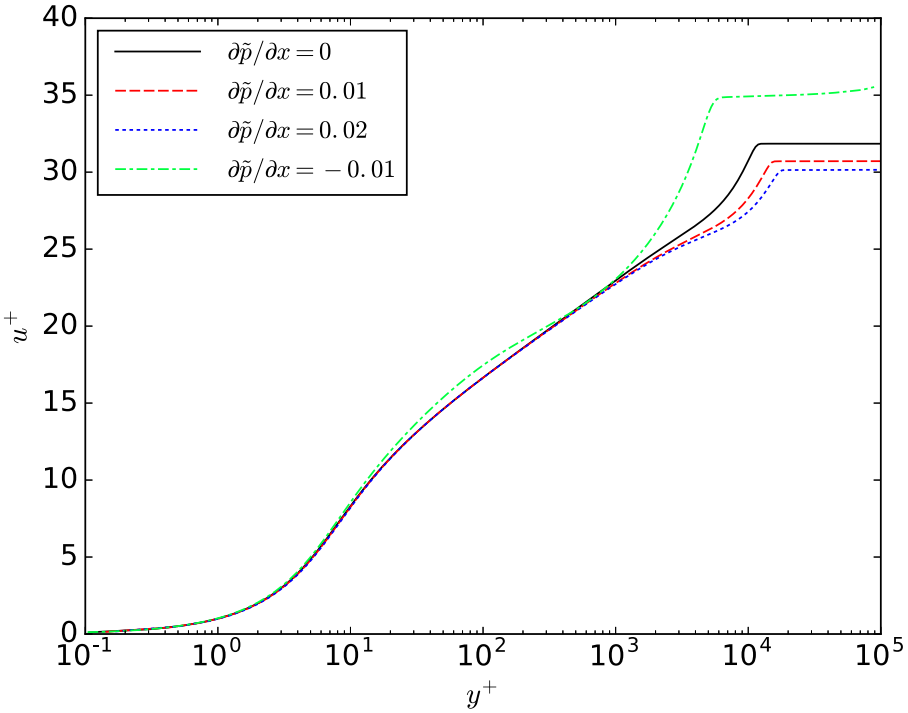

$M_\infty = 0.30$

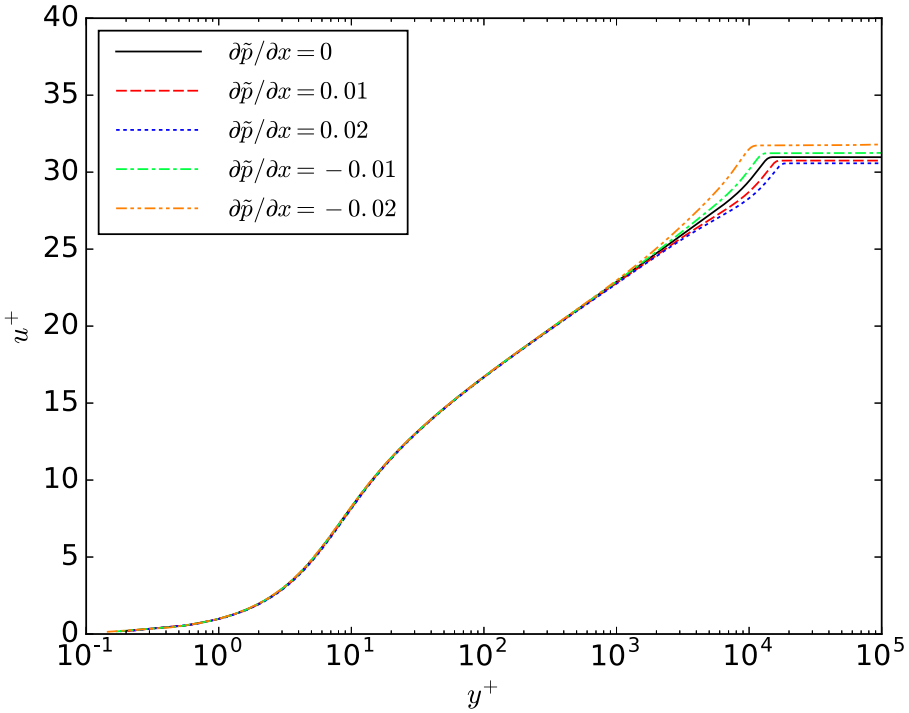

$M_\infty = 0.50$

Variation of u^+ in Inner Coordinates as Function of M_∞ and $\partial \tilde{p}/\partial x$

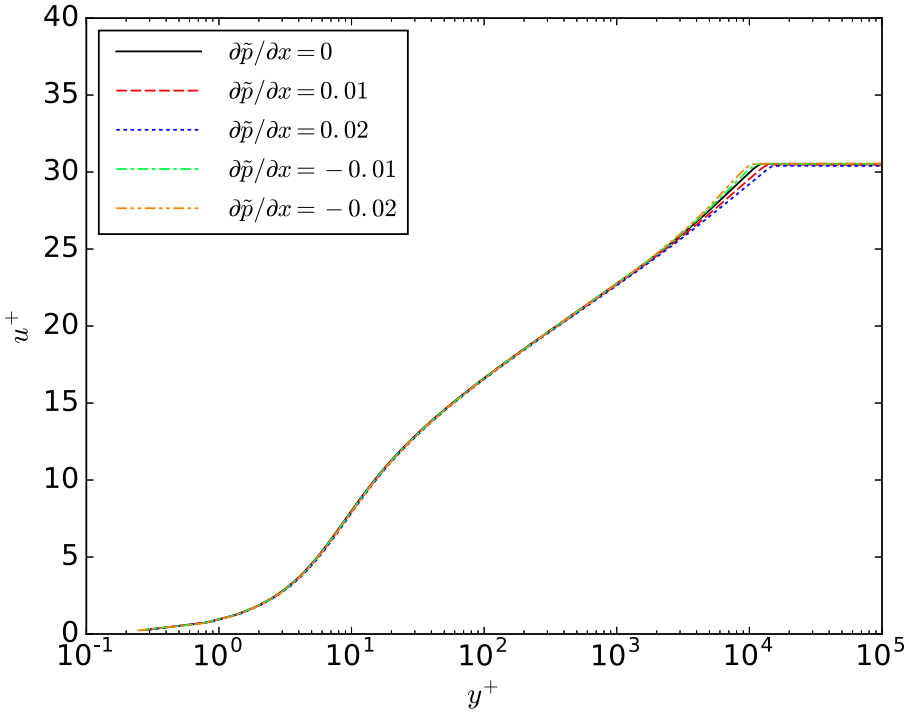

$M_\infty = 0.70$

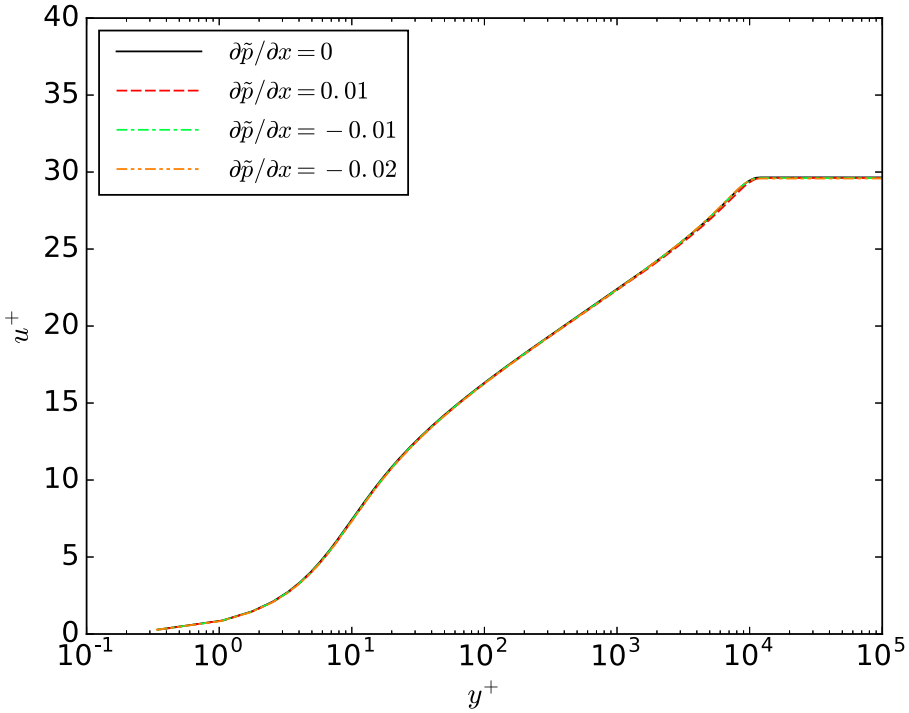

$M_\infty = 0.90$

Variation of ρ and T in Inner Coordinates for Various M_∞

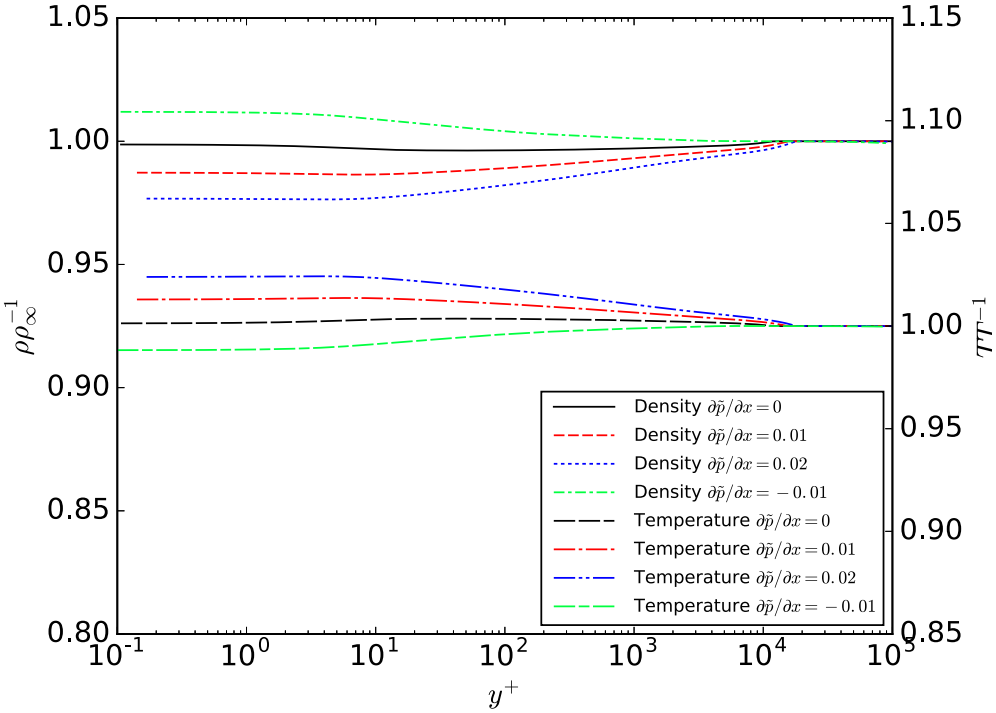

$M_\infty = 0.30$

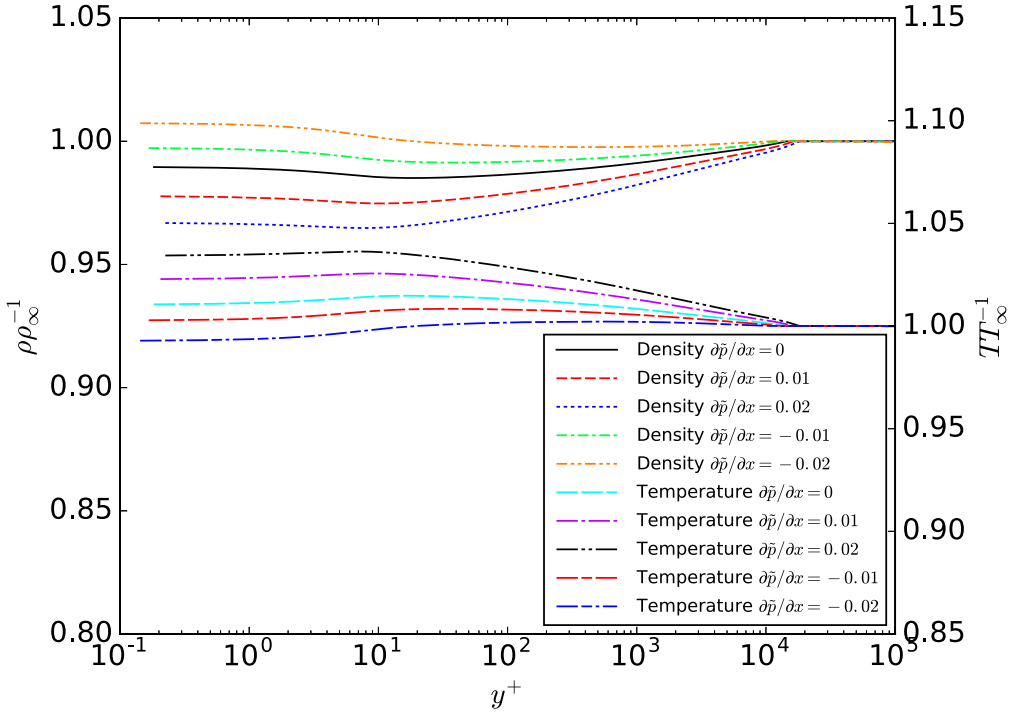

$M_\infty = 0.50$

Variation of ρ and T in Inner Coordinates for Various M_∞

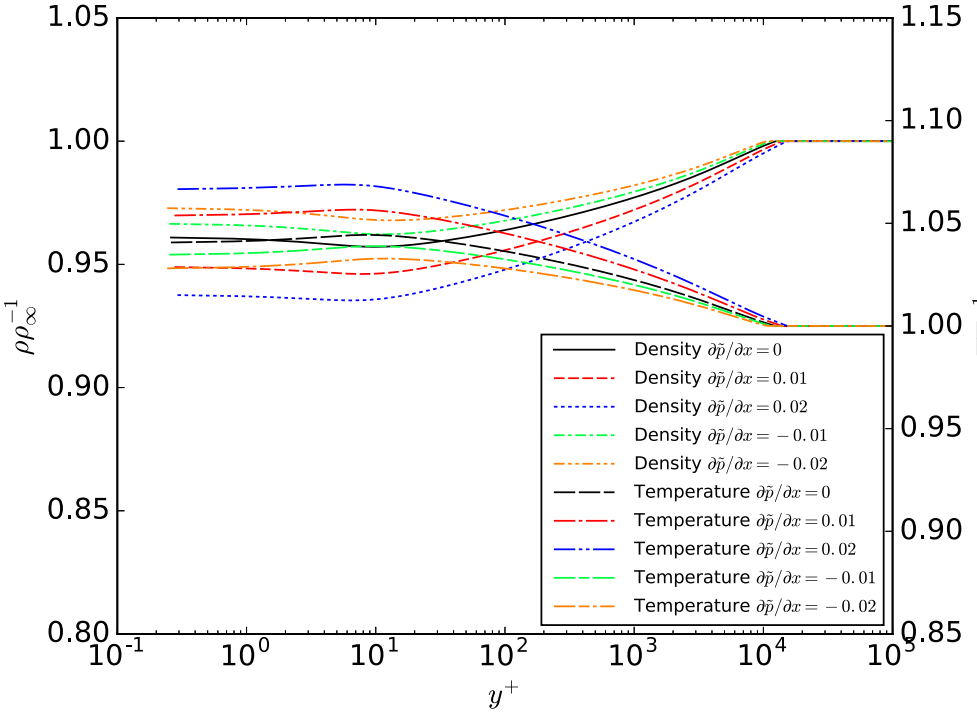

$M_\infty = 0.70$

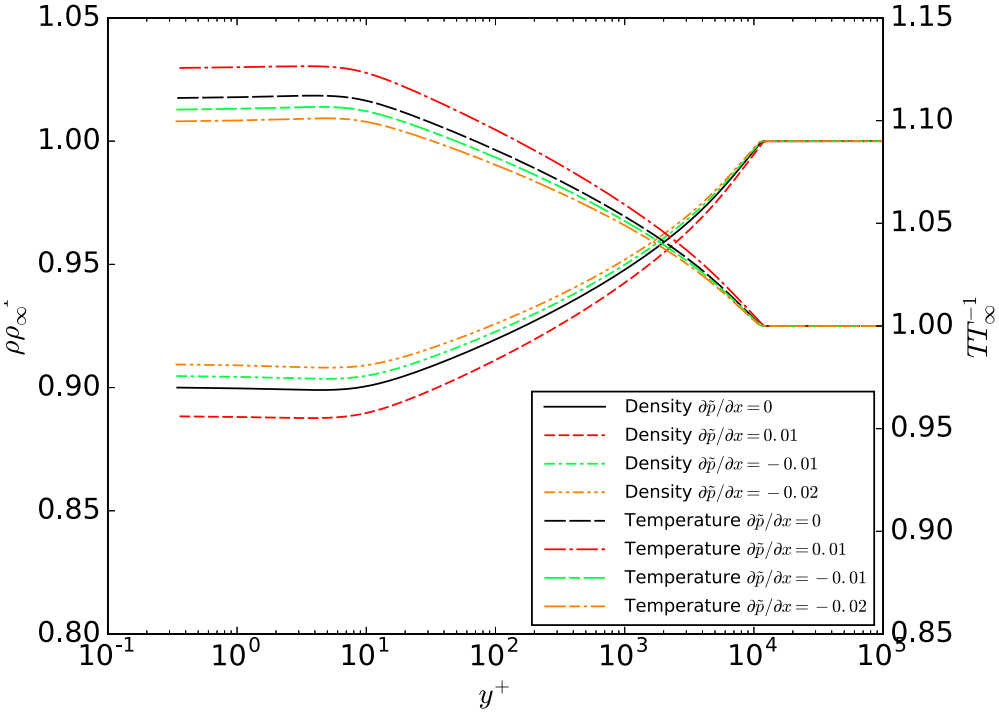

$M_\infty = 0.90$

Normalized Variation of u_{rms} in Inner Coordinates

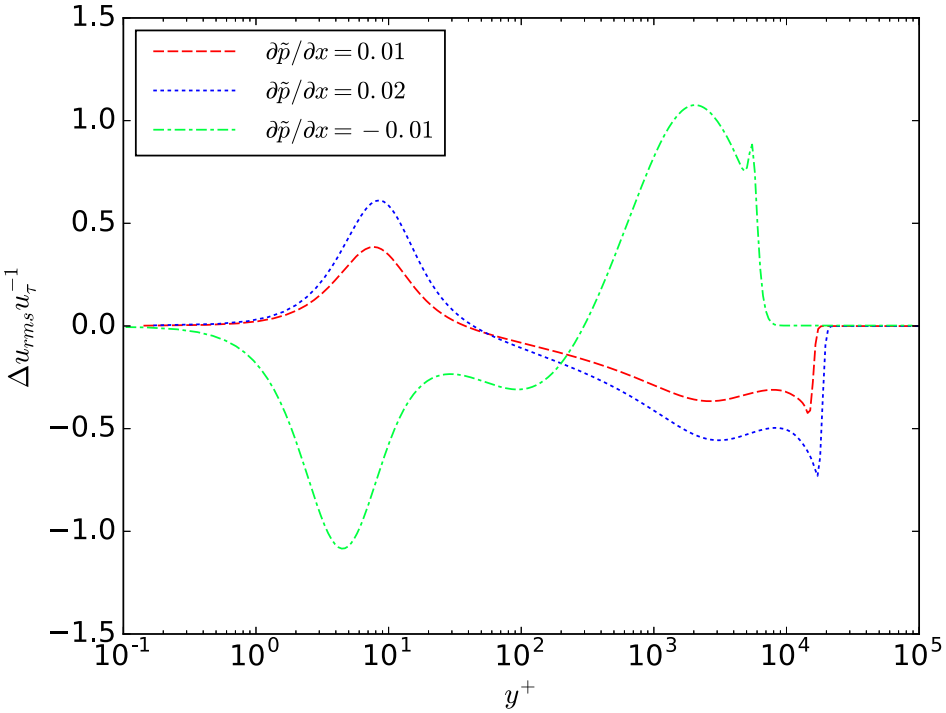

$M_\infty = 0.30$

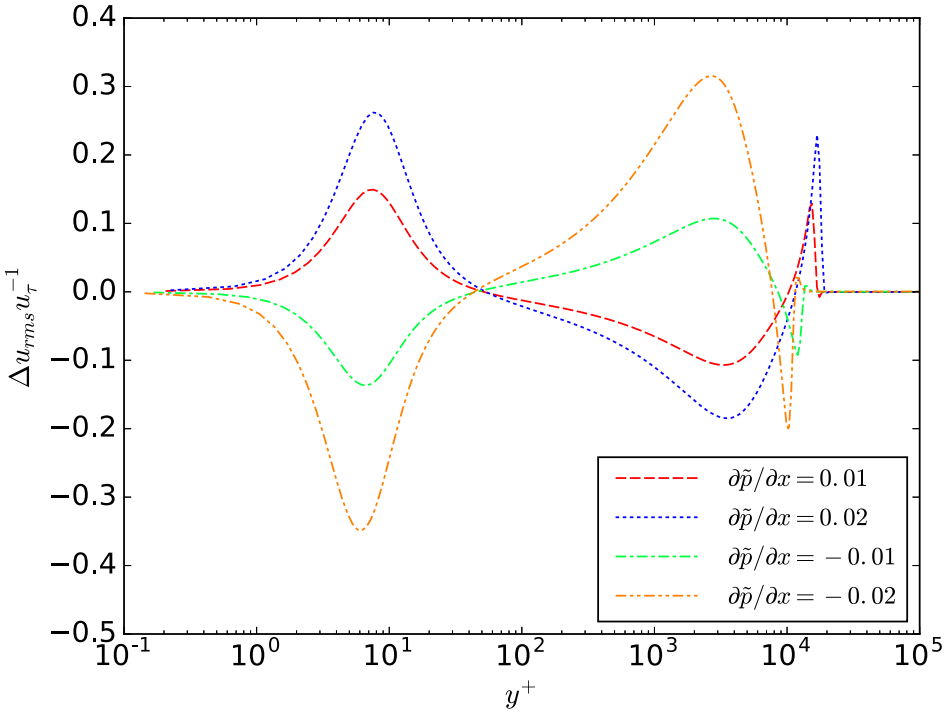

$M_\infty = 0.50$

Normalized Variation of u_{rms} in Inner Coordinates

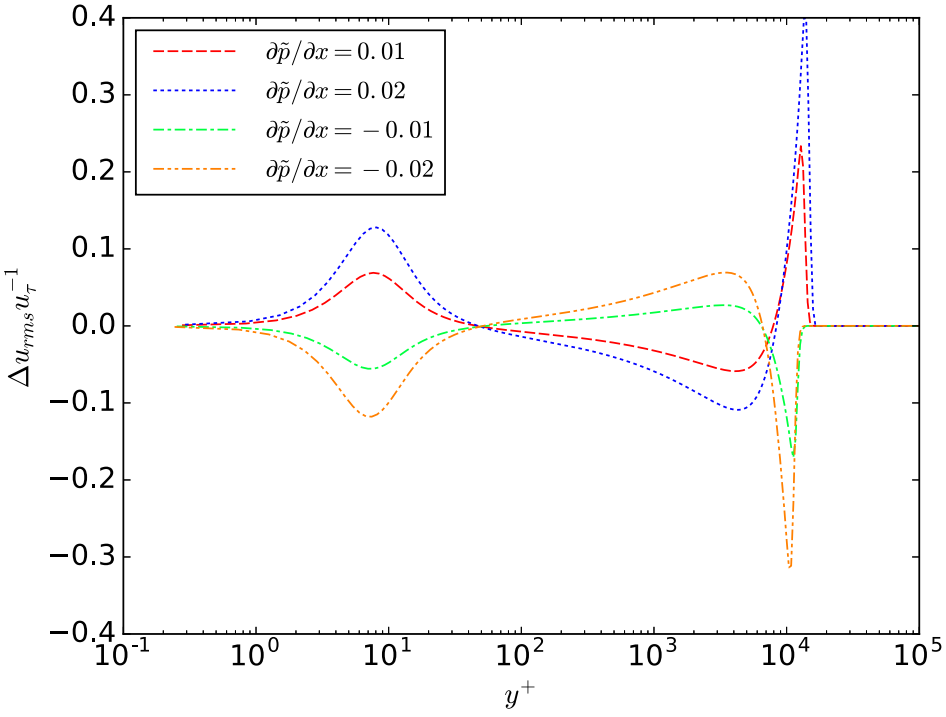

$M_\infty = 0.70$

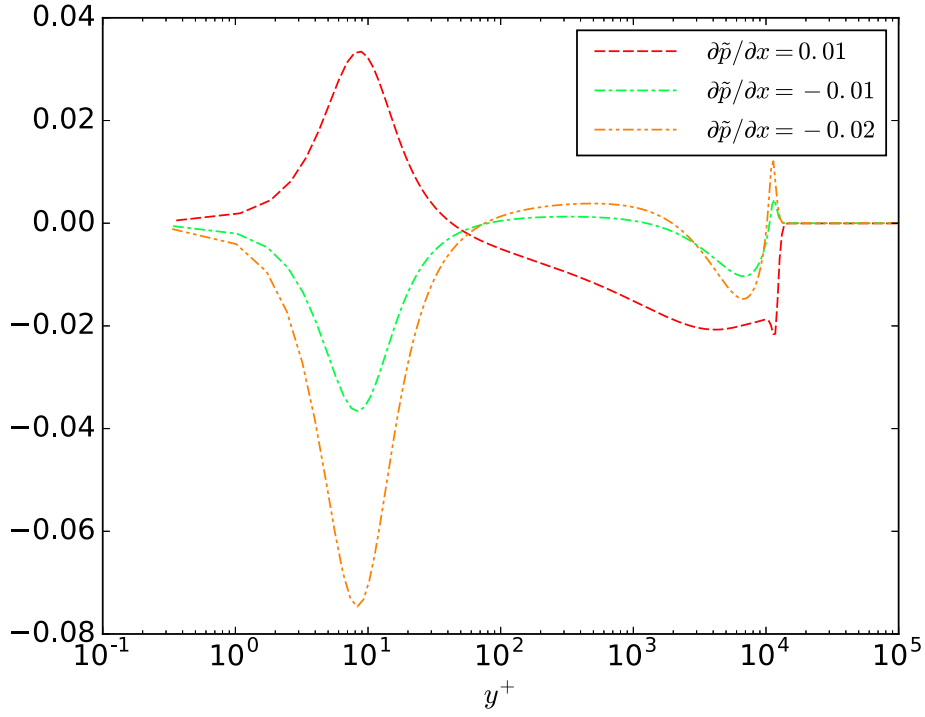

$M_\infty = 0.90$

Normalized Variation of the Root Mean of *uv* in Inner Coordinates

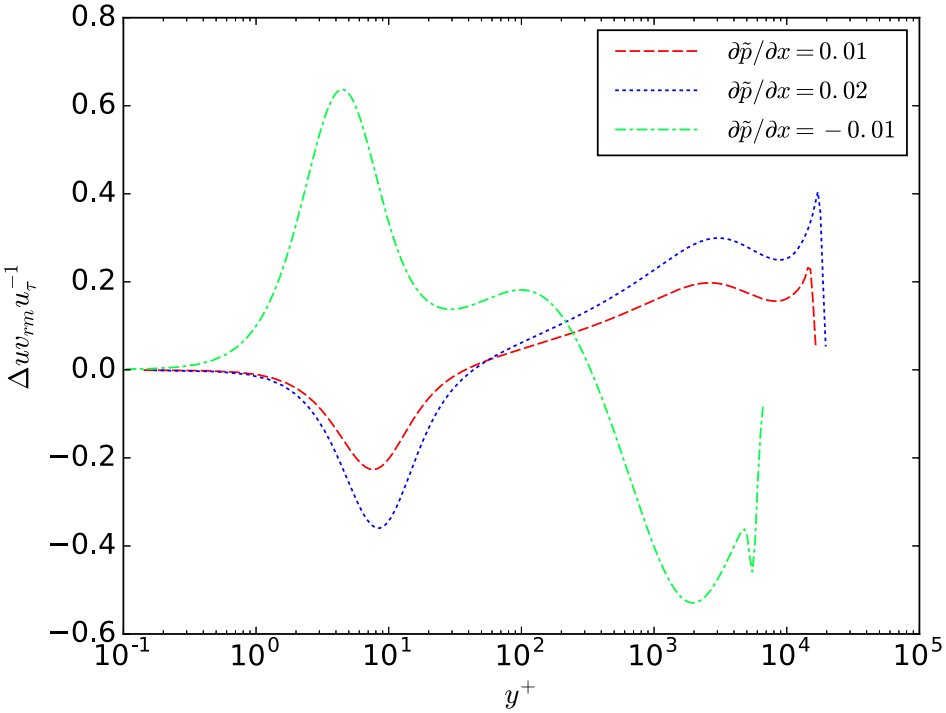

$M_\infty = 0.30$

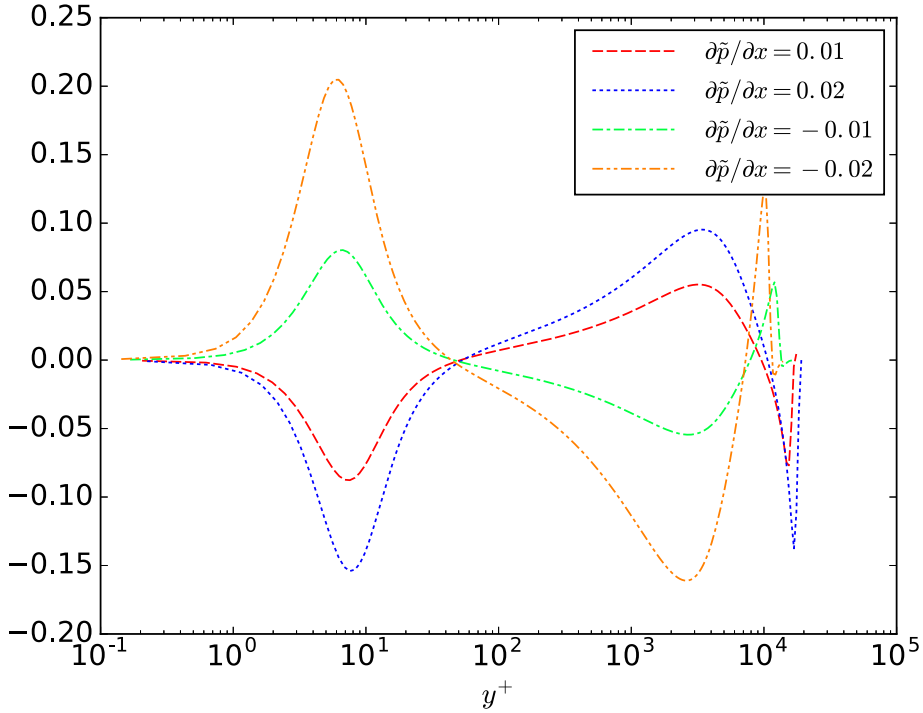

$M_\infty = 0.50$

Normalized Variation of the Root Mean of *uv* in Inner Coordinates

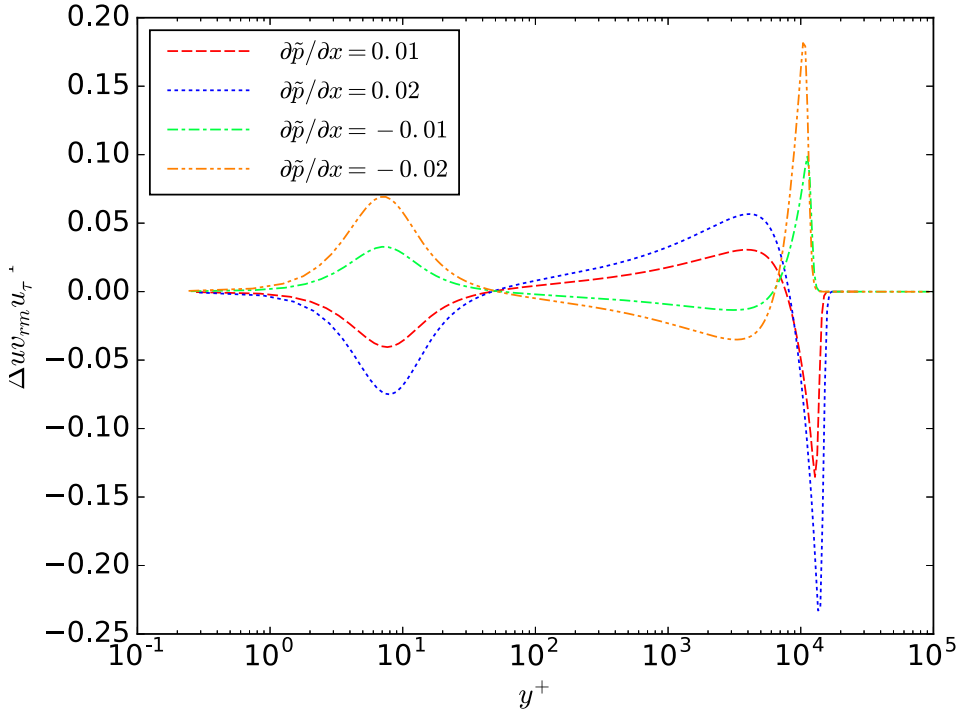

$M_\infty = 0.70$

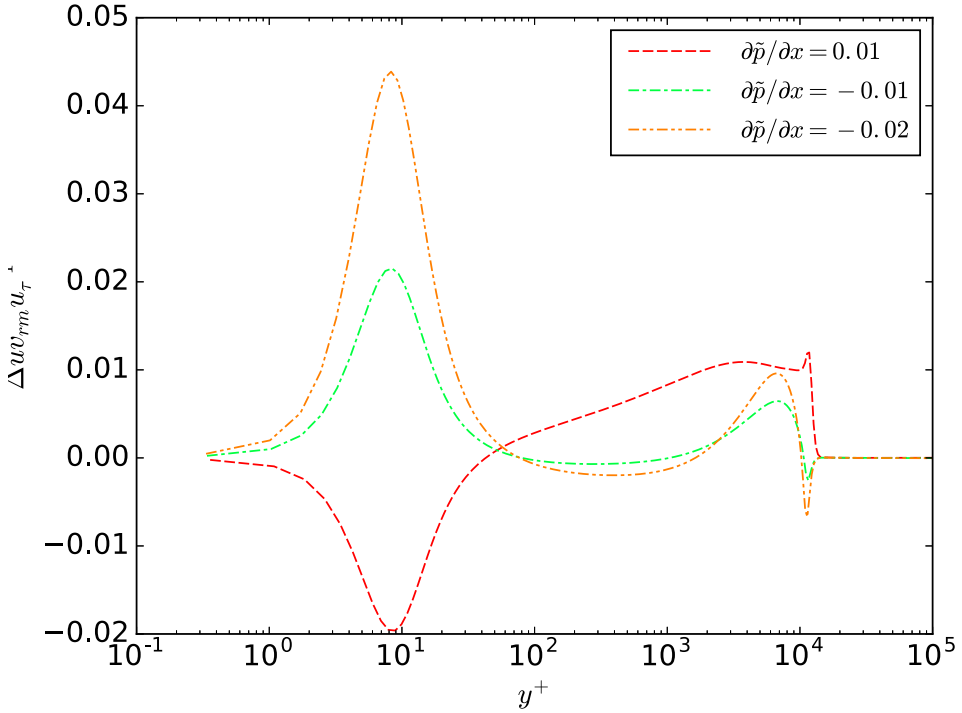

$M_\infty = 0.90$

Comparison of the Newly Developed Prediction Approach with the Predictions of Miller and the LES Predictions of Gloerfelt and Margnat

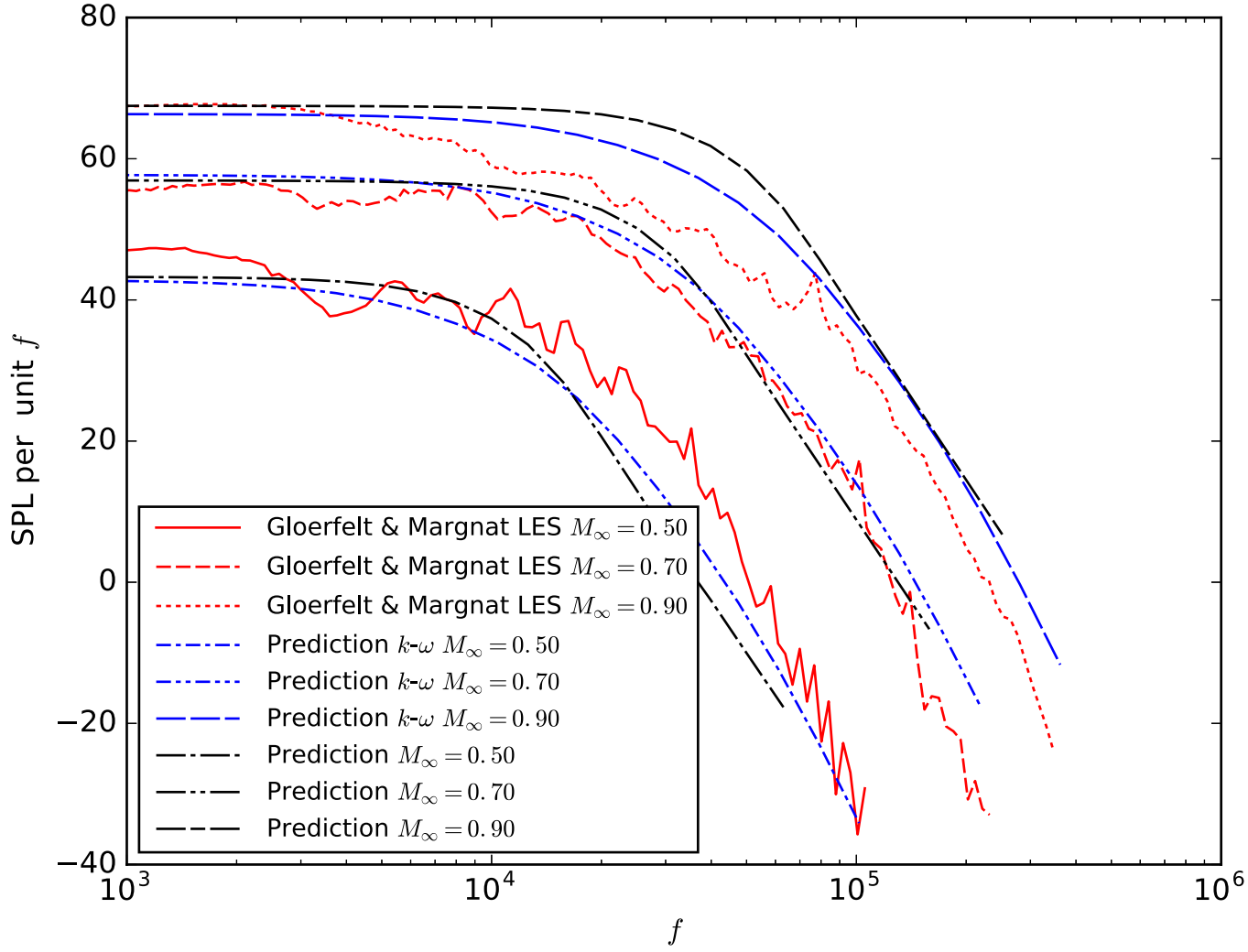

Predictions of SPL per unit f with Various M_∞ and $\partial\tilde{p}/\partial x$

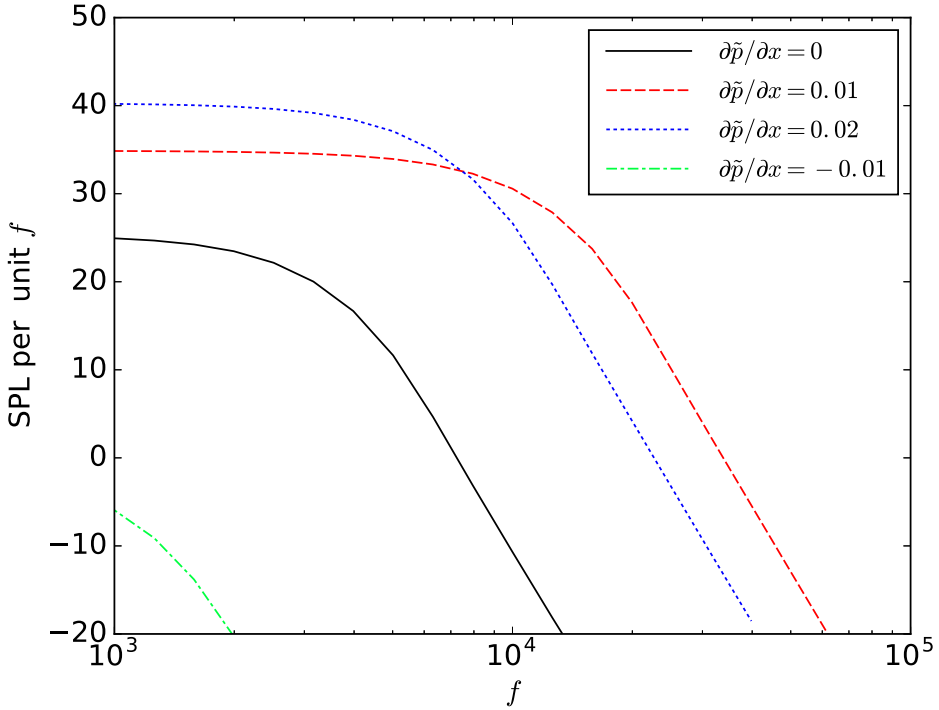

$M_\infty = 0.30$

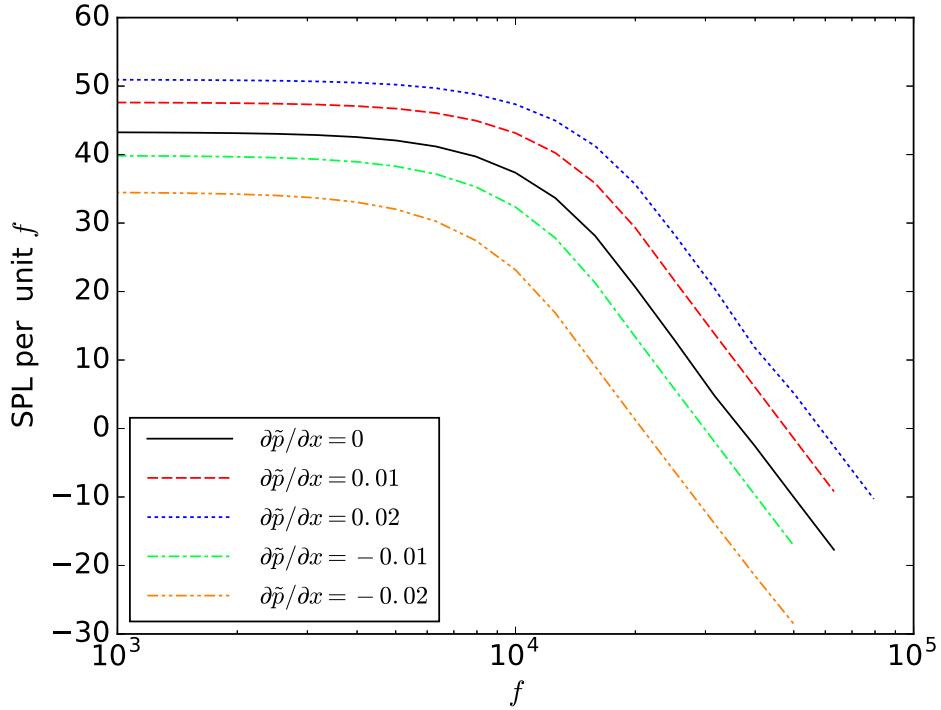

$M_\infty = 0.50$

Predictions of SPL per unit f with Various M_∞ and $\partial\tilde{p}/\partial x$

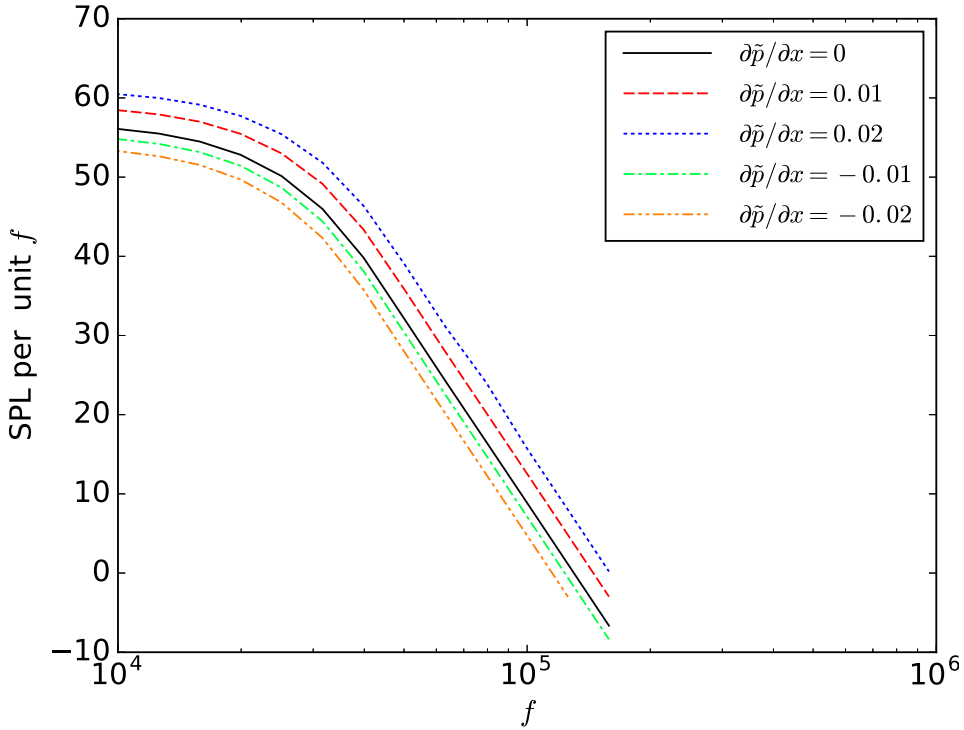

$M_\infty = 0.70$

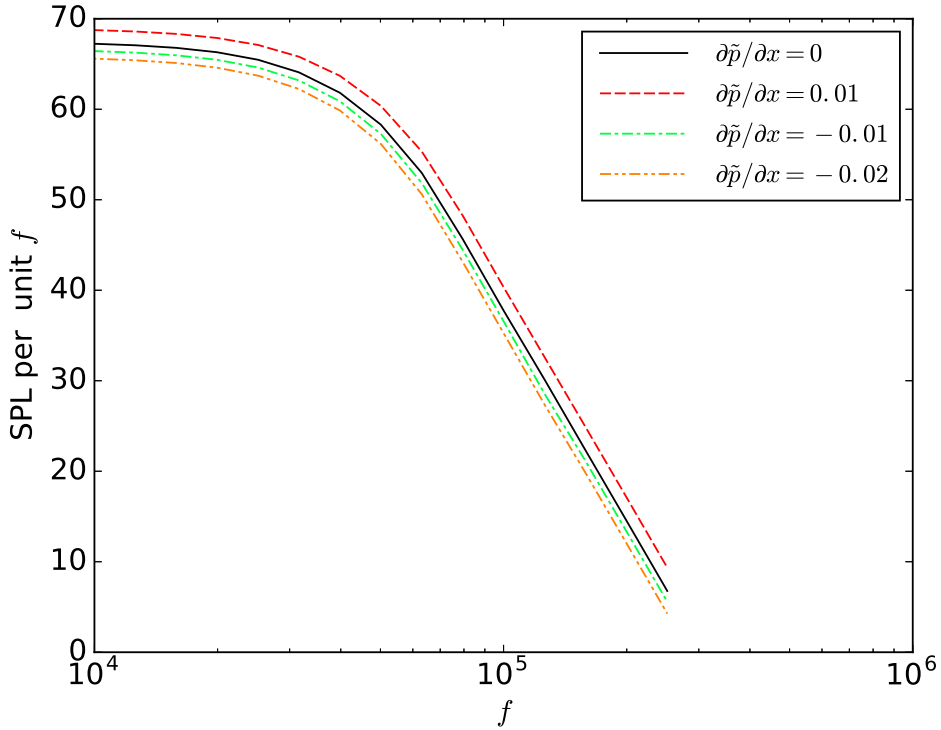

$M_\infty = 0.90$

Summary and Conclusion

Summary and Conclusion

- Acoustic analogy connected to RANS algebraic Reynolds stress model
- Predictions agree with previous analytical model and well validated LES

- Important findings
  - At low Mach numbers the statistics of turbulence, meanflow, and acoustic radiation are highly affected by pressure gradient relative to high Mach number subsonic flows
  - Small negative incremental steps in non-dimensional pressure gradient produce lower energy acoustic power spectra
  - Spectra shift to lower frequencies and sound pressure levels with favorable pressure gradients

- Development of composite meanflow profiles and similarity of turbulent statistics with pressure gradient would allow a fully statistical model to be developed that does not rely on CFD

Thank You

Questions?

Modeling the Equivalent Source

We need to create models for,

$$\overline{T_{ij}T'_{lm}} \qquad \text{and,} \qquad \overline{\dot{T}_{ij}\dot{T}'_{lm}} \qquad \text{and,} \qquad \overline{\ddot{T}_{ij}\ddot{T}'_{lm}}$$

We define,

$$\overline{T_{ij}T'_{lm}} = R_{ijlm}(\boldsymbol{y}_1, \boldsymbol{\eta}, \tau)$$

and argue based on the principles of Millionshchikov, M. D.,

$$\overline{\frac{\partial^2}{\partial\tau_1^2}T_{ij}\frac{\partial^2}{\partial\tau_2^2}T'_{lm}} = \frac{\partial^4}{\partial\tau^4}T_{ijlm}(\boldsymbol{\eta}, \boldsymbol{\xi}, \tau) = \frac{\partial^4}{\partial\tau^4}R_{ijlm}(\boldsymbol{y}_1, \boldsymbol{\eta}, \tau)$$

and,

$$\overline{\frac{\partial}{\partial\tau_1}T_{ij}\frac{\partial}{\partial\tau_2}T'_{lm}} = \frac{\partial^2}{\partial\tau^2}T_{ijlm}(\boldsymbol{\eta}, \boldsymbol{\xi}, \tau) = \frac{\partial^2}{\partial\tau^2}R_{ijlm}(\boldsymbol{y}_1, \boldsymbol{\eta}, \tau)$$

Thus, we only need to model $\overline{T_{ij}T'_{lm}}$ as they are inter-related, (eg what is R_{ijlm})?,